ACS NANO
Cite This: ACS Nano XXXX, XXX, XXX−XXX
www.acsnano.org

ARTICLE

Multilamellar Vaccine Particle Elicits Potent Immune Activation with Protein Antigens and Protects Mice against Ebola Virus Infection

Yuchen Fan,[†,‡] Sabrina M. Stronsky,[§,#] Yao Xu,[†,‡] Jesse T. Steffens,[§] Sean A. van Tongeren,[§] Amanda Erwin,[⊥] Christopher L. Cooper,[*,§] and James J. Moon[*,†,‡,∥]

[†]Department of Pharmaceutical Sciences, University of Michigan, Ann Arbor, Michigan 48109, United States
[‡]Biointerfaces Institute, University of Michigan, Ann Arbor, Michigan 48109, United States
[§]Molecular and Translational Sciences, United States Army Medical Research Institute of Infectious Diseases (USAMRIID), Fort Detrick, Maryland 21702, United States
[#]Joint Program Executive Office - Chemical, Biological, Radiological, and Nuclear Defense (JPEO−CBRND), Fort Detrick, Maryland 21702, United States
[⊥]Department of Cell and Developmental Biology, University of Michigan, Ann Arbor, Michigan 48109, United States
[∥]Department of Biomedical Engineering, University of Michigan, Ann Arbor, Michigan 48109, United States

Supporting Information

ABSTRACT: **Recent outbreaks of emerging infectious diseases, such as Ebola virus disease (EVD), highlight the urgent need to develop effective countermeasures, including prophylactic vaccines. Subunit proteins derived from pathogens provide a safe source of antigens for vaccination, but they are often limited by their low immunogenicity. We have developed a multilamellar vaccine particle (MVP) system composed of lipid−hyaluronic acid multi-cross-linked hybrid nanoparticles for vaccination with protein antigens and demonstrate their efficacy against Ebola virus (EBOV) exposure. MVPs efficiently accumulated in dendritic cells and promote antigen processing. Mice immunized with MVPs elicited robust and long-lasting antigen-specific $CD8^+$ and $CD4^+$ T cell immune responses as well as humoral immunity. A single-dose vaccination with MVPs delivering EBOV glycoprotein achieved an 80% protection rate against lethal EBOV infection. These results suggest that MVPs offer a promising platform for improving recombinant protein-based vaccine approaches.**

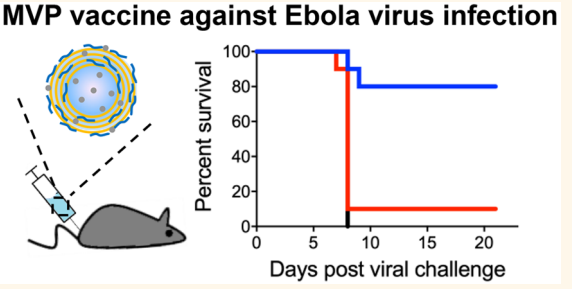

KEYWORDS: *subunit vaccine, nanoparticle, hyaluronic acid, liposome, Ebola*

Emerging infectious pathogens, such as Ebola virus (EBOV) and Zika virus, have caused a severe burden on public health, as evidenced by recent outbreaks.[1,2] As prophylactic vaccines have controlled or even eradicated several deadly pathogens in human history,[3] successful vaccines would provide effective countermeasures against new emerging infectious pathogens. Viral vector-based EBOV vaccines, such as recombinant vesicular stomatitis virus (rVSV), have achieved promising disease protection rates in the field.[4−6] Yet, there are still concerns of pre-existing immunity, undesired reactogenicity, and safety issues associated with traditional vaccine approaches.[5−9] Molecularly defined subunit protein antigens can offer safer alternatives with less complicated manufacturing processes. However, on the other hand, soluble protein antigens are susceptible to deactivation or degradation, and they are less immunogenic than live vector vaccines. While various nanoparticle systems have been developed for delivery of subunit antigens to antigen-presenting cells (APCs) to induce adaptive immune responses,[10−12] it remains challenging to achieve robust, long-lasting, and concerted cellular and humoral immune responses with protein antigens.

In this work, we sought to address these issues by developing a lipid/biopolymer hybrid nanovaccine system that can deliver protein antigens to dendritic cells (DCs), promote antigen presentation, and generate CD8+ and CD4+ T cell as well as humoral immune responses in a concerted manner. We have previously reported a multilamellar lipid nanosystem formed

Received: May 11, 2019
Accepted: September 9, 2019
Published: September 9, 2019

DOI: 10.1021/acsnano.9b03660
ACS Nano XXXX, XXX, XXX−XXX

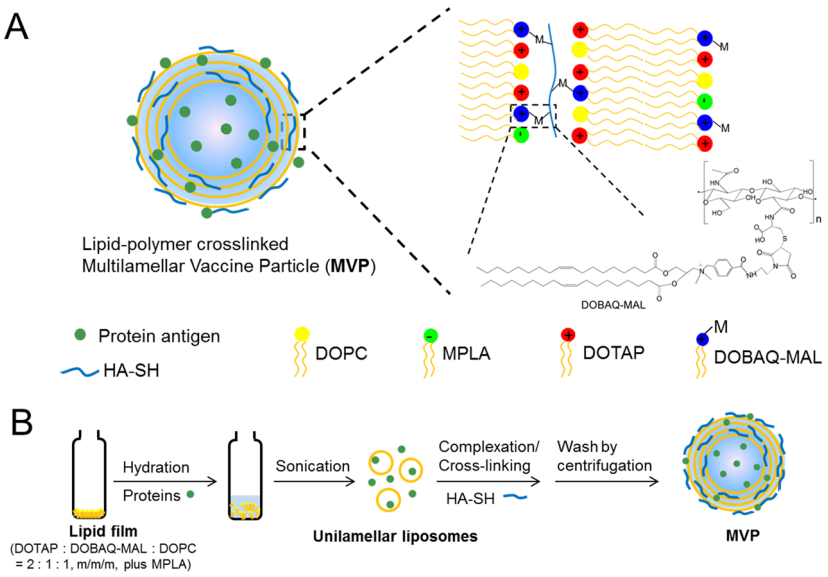

Figure 1. (A) Schematic of multilamellar vaccine particles (MVPs) coloaded with protein antigen and MPLA. (B) Synthesis of MVPs. Lipid film is hydrated to form unilamellar liposomes containing maleimide-modified cationic lipids. Liposomes are then complexed and cross-linked by multithiolated hyaluronic acid (HA-SH), thereby forming MVPs.

by cross-linking of phospholipids within lipid vesicles using a bifunctional cross-linker and shown their utility for vaccine applications.[13−17] In a separate line of work, we have also reported a vaccine delivery vehicle formed by complexation of 1,2-dioleoyl-3-trimethylammonium-propane (DOTAP) liposome−hyaluronic acid.[18] Here, we sought to combine these two approaches by developing a lipid−polymer hybrid multilamellar vaccine particle (MVP) that is stabilized by multi-cross-linking of maleimide-displaying lipid bilayers with thiolated hyaluronic acid (HA-SH) (Figure 1. We chose hyaluronic acid (HA) as our biopolymer multi-cross-linker since HA is anionic for promoting fusion of cationic liposomes into multilamellar vesicles,[18] biocompatible, and used widely in FDA-approved products.[19] Here, we demonstrate that MVPs can be stably coloaded with protein antigens and monophosphoryl lipid A (MPLA), a Toll-like receptor (TLR) 4 agonist approved for use in vaccine products,[20,21] and that MVPs efficiently activate DCs and promote antigen processing. Using ovalbumin (OVA) as the model antigen, we show that immunizations with MVPs carrying OVA and MPLA induce robust expansion of OVA-specific $CD8^+$ and $CD4^+$ T cells and elicit durable cellular and humoral immune responses *in vivo*. To assess the efficacy of MVPs against EBOV, we performed immunization studies with MVPs carrying EBOV glycoprotein (GP), a recombinant protein antigen derived from the viral spike glycoprotein.[22−25] MVPs coloaded with GP and MPLA significantly enhanced GP-specific T cell immune responses, compared with soluble vaccination. Impressively, a single vaccine dose of MVPs protected 80% of mice against a lethal EBOV exposure. These results show that MVP is a promising delivery platform for subunit protein antigens and may serve as a potent delivery system for vaccination against emerging pathogens.

RESULTS AND DISCUSSION

MVPs Stably Encapsulate and Display Protein Antigens. We have developed multilamellar vaccine particles (Figure 1A) designed for stable presentation and delivery of protein antigens and adjuvant molecules in order to generate robust and durable humoral and cellular immune responses. Briefly, MVPs were synthesized by hydrating a lipid film in the presence of protein antigens and adjuvant molecules to form unilamellar liposomes, followed by incubation with biopolymers to fuse and cross-link lipid bilayers within lipid vesicles (Figure 1B). Specifically, a lipid film composed of DOTAP—maleimide-functionalized *N*-(4-carboxybenzyl)-*N*,*N*-dimethyl-2,3-bis(oleoyloxy)propan-1-aminium (DOBAQ)/1,2-dioleoyl-*sn*-glycero-3-phosphocholine (DOPC), 2:1:1, m/m/m)—was hydrated and sonicated to form unilamellar liposomes displaying cationic, maleimide-functionalized lipid layers with an initial size of 130 ± 20 in diameter (Table S1). Resulting liposomes were then incubated with anionic HA polymer premodified with multiple pendant thiols (HA-SH) (Figure 1B). Addition of HA-SH promoted complexation of hydrated liposomes into multilamellar vesicles and formation of lipid−HA hybrid MVPs (Figure 1B). MPVs formed with MPLA added to the initial lipid film exhibited a hydrodynamic size of 230 ± 10 nm, while OVA, a model antigen, added during the initial liposome formation further increased the size of OVA/MPLA MVPs to 280 ± 40 nm in diameter with a polydispersity index of 0.18 ± 0.03 (Table S1). MVPs coloaded with EBOV GP and MPLA showed an increased particle size of 350 ± 5 nm in diameter (Table S1), possibly due to the higher molecular weight of GP antigen compared to OVA (MW of GP monomer 150 kDa; MW of OVA 43 kDa). Notably, the initial cationic surface charge of 19.5 ± 0.2 mV for unilamellar liposomes turned to −17.8 ± 0.4 mV after complexation with HA-SH (Table S1). Lamellarity measurement[26] showed that the fraction of lipid exposed on the external surface decreased from 0.57 ± 0.01 for unilamellar liposomes to 0.39 ± 0.02 for MVPs (Table S2), indicating multilamellar nanostructure of MVPs.

Next, we measured the encapsulation efficacy (EE%) of protein antigens in MVPs using sodium dodecyl sulfate polyacrylamide gel electrophoresis (SDS-PAGE), followed by Coomassie blue staining. Mean EE% of OVA and GP in MVPs were ∼18% and ∼36%, corresponding to ∼9 μg of OVA and ∼15 μg of GP per mg of lipid, respectively (Table S3).

DOI: 10.1021/acsnano.9b03660
ACS Nano XXXX, XXX, XXX−XXX

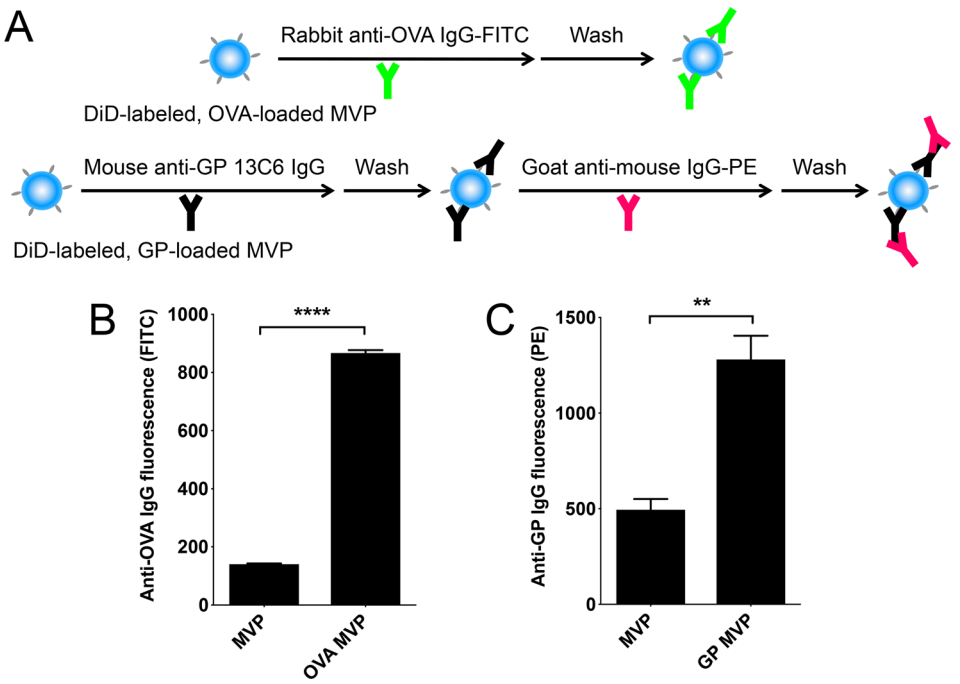

Figure 2. Surface display of antigens on the surface of MVPs. (A) Experimental scheme. Protein-loaded and DiD-labeled MVPs were stained by a fluorophore-labeled, anti-OVA primary antibody or an anti-Ebola GP primary antibody and a fluorophore-labeled secondary antibody, followed by quantification of the fluorescence intensity between MVP with or without antigen. Results are presented as mean ± SEM, $n = 3$. $^{**}P < 0.01$, $^{****}P < 0.0001$, analyzed by unpaired, two-tailed Student's *t*-test.

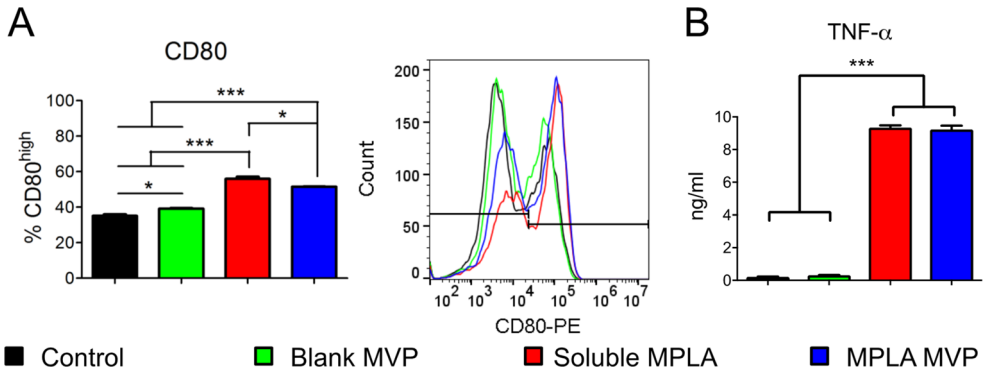

Figure 3. MPLA-loaded MVPs activate DCs *in vitro*. (A) BMDCs were treated with soluble MPLA or MVPs with or without MPLA for 24 h, followed by the measurement of CD80 expression on BMDCs by flow cytometry. Representative histograms are shown. (B) Cell culture supernatant was also collected for the measurement of TNF-α by ELISA. Results are presented as mean ± SEM, $n = 3$. $^{*}P < 0.05$, $^{**}P < 0.01$, $^{***}P < 0.001$, analyzed by one-way ANOVA with the Bonferroni multiple comparison post-test.

Furthermore, we observed only ~10% leakage of OVA from MVPs incubated in 10% fetal bovine serum (FBS)-containing phosphate-buffered saline (PBS) over 7 days (Figure S1), and upon exposure to Triton X-100 detergent, MVPs retained antigens significantly more effectively than liposomes of similar lipid composition (Figure S2), thus indicating stability of antigen-loaded MVPs.

Since recognition and internalization of antigens by B cell receptors is the prerequisite for B cell activation and production of antigen-specific antibodies, we examined whether protein antigens were properly displayed on the surfaces of MVPs by an immunofluorescence assay (Figure 2A). Briefly, we measured the fluorescence signal of anti-OVA or anti-EBOV GP antibodies directed against surface antigens on MVPs and then normalized the fluorescence intensity to the particle retention (as measured by the recovery of 1,1′-dioctadecyl-3,3,3′,3′-tetramethylindodicarbocyanine (DiD) embedded within MVPs as a marker for particle yield, Figure 2A). MVPs loaded with OVA were readily detected with anti-OVA IgG, showing a 6-fold increase in antibody binding compared with blank MVPs ($P < 0.0001$, Figure 2B). Similarly, MVPs loaded with EBOV GP showed a 2.6-fold increase in surface binding of a conformational anti-GP antibody, 13C6, that binds to a quaternary epitope within the GP_1/GP_2 glycan cap[27,28] ($P < 0.01$, Figure 2C, Figure S3). These results indicated that a subset of protein antigen encapsulated in MVPs was exposed on the particle surface and the surface-displayed antigens were readily accessible to configurational antibodies, which would allow for induction of antigen-specific humoral immune responses *in vivo*.[29] While we could not detect antigen displayed on MVPs under transmission electron microscopy (Figure S4), GP retrieved from MVPs exhibited higher MW compared with GP standards when analyzed by

DOI: 10.1021/acsnano.9b03660
ACS Nano XXXX, XXX, XXX−XXX

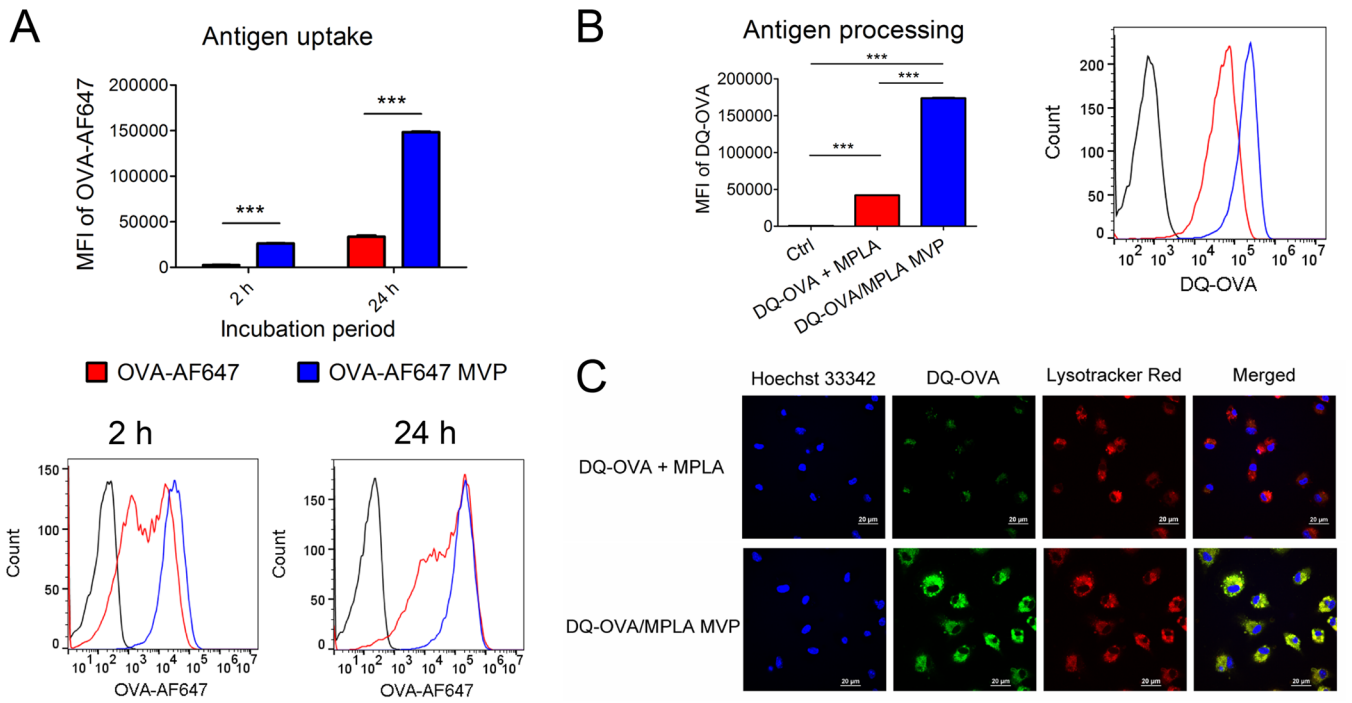

Figure 4. MVP promotes antigen uptake and processing by DCs *in vitro*. (A) BMDCs were treated with OVA-AF647 or OVA-AF647-loaded MVPs for 2 or 24 h, followed by the measurement of antigen uptake by flow cytometry. Representative histograms are shown. (B, C) BMDCs were treated with the soluble mixture of DQ-OVA and MPLA or DQ-OVA/MPLA MVPs for 24 h, followed by the measurement of fluorescence intensity by (B) flow cytometry or (C) confocal microscopy. (C) Nuclei and lysosomes were stained with Hoechst 33342 and Lysotracker Red, respectively. Scale bars = 20 μm. Results in (A) and (B) are shown as mean ± SEM, $n = 3$. ***$P < 0.001$, analyzed by two-way (A) or one-way (B) ANOVA with the Bonferroni multiple comparison post-test.

SDS-PAGE (Figure S5), suggesting conjugation of maleimide-displaying lipids with free thiols in proteins.

MVPs Increase Antigen Accumulation and Processing by DCs. We first examined MVP-mediated DC activation *in vitro*. Bone-marrow-derived dendritic cells (BMDCs) incubated with either soluble MPLA or MPLA-loaded MVPs increased the expression levels of CD80, a co-stimulatory marker (Figure 3A), and promoted DC secretion of TNF-α (Figure 3B), compared with BMDCs incubated with PBS or blank MVPs, showing that MVPs decorated with MPLA can activate DCs.

Since antigen uptake and antigen process by APCs are both critical steps for the initiation of antigen-specific T cell responses,[30] we examined cellular uptake of OVA as a soluble or MVP form using BMDCs. After 2 h of incubation of BMDCs with OVA tagged with AF647, MVPs increased DC uptake of OVA by 10-fold, compared with soluble OVA, as shown by the mean fluorescence intensity (MFI) of OVA-AF647 among DCs and their representative flow cytometry histograms ($P < 0.001$, Figure 4A). After 24 h, we still observed a 4.4-fold enhancement in OVA uptake of MVPs, compared with soluble OVA ($P < 0.001$, Figure 4A). We next examined the impact of MVP-mediated antigen delivery on intracellular antigen processing. MVPs were coloaded with MPLA and DQ-OVA, which is OVA protein labeled with self-quenched fluorescent dyes that fluoresce upon protease-mediated degradation.[31] Compared with the soluble mixture of DQ-OVA + MPLA, MVPs significantly enhanced the intracellular processing of DQ-OVA, as evidenced by a 4-fold increase in the DQ-OVA fluorescence measured by flow cytometric analysis after 24 h of BMDC culture ($P < 0.001$, Figure 4B). We further confirmed these results with confocal microscopy; whereas BMDCs pulsed with a soluble DQ-OVA + MPLA mixture displayed weak DQ-OVA fluorescence signal after 24 h, BMDCs treated with MVPs exhibited strong DQ-OVA fluorescence signal from endolysosomes and throughout the cytosol (Figure 4C). Taken together, these results suggested that MVPs increased antigen delivery to DCs and promoted antigen processing by DCs.

MVPs Elicit Strong and Durable Antigen-Specific T Cell Immune Responses *in Vivo*. We assessed the impact of MVP vaccination on induction of antigen-specific T cell responses. Naïve C57BL/6 mice were immunized subcutaneously at the tail base on weeks 0, 3, and 6 and examined for antigen-specific $CD8^+$ and $CD4^+$ T cell responses by IFN-γ^+ ELISPOT (Figure 5A). Seven days after the first and second vaccination, we observed that OVA/MPLA MVPs elicited 20-fold and 11-fold higher levels of OVA-I specific splenic $CD8^+$ T cell responses, compared with the soluble mixture of OVA and MPLA ($P < 0.001$, Figure 5B,C). To examine the durability of antigen-specific T cell immune responses, we administered the third vaccination and waited 4 months prior to performing the ELISPOT assay. Animals immunized with the MVP vaccine maintained significantly higher OVA-specific $CD8^+$ T cell responses as demonstrated by a 4-fold greater average number of ELISPOT counts, compared with the soluble vaccine ($P < 0.05$, Figure 5D). We also confirmed systemic $CD8^+$ T cell responses by SIINFEKL-$H2K^b$-tetramer staining of peripheral blood mononuclear cells (PBMCs) (Figure S6). In stark contrast, throughout the study, animals immunized with the soluble OVA + MPLA vaccine failed to induce statistically significant antigen-specific $CD8^+$ T cell responses, compared with the PBS control group (Figure 5B–D).

DOI: 10.1021/acsnano.9b03660
ACS Nano XXXX, XXX, XXX−XXX

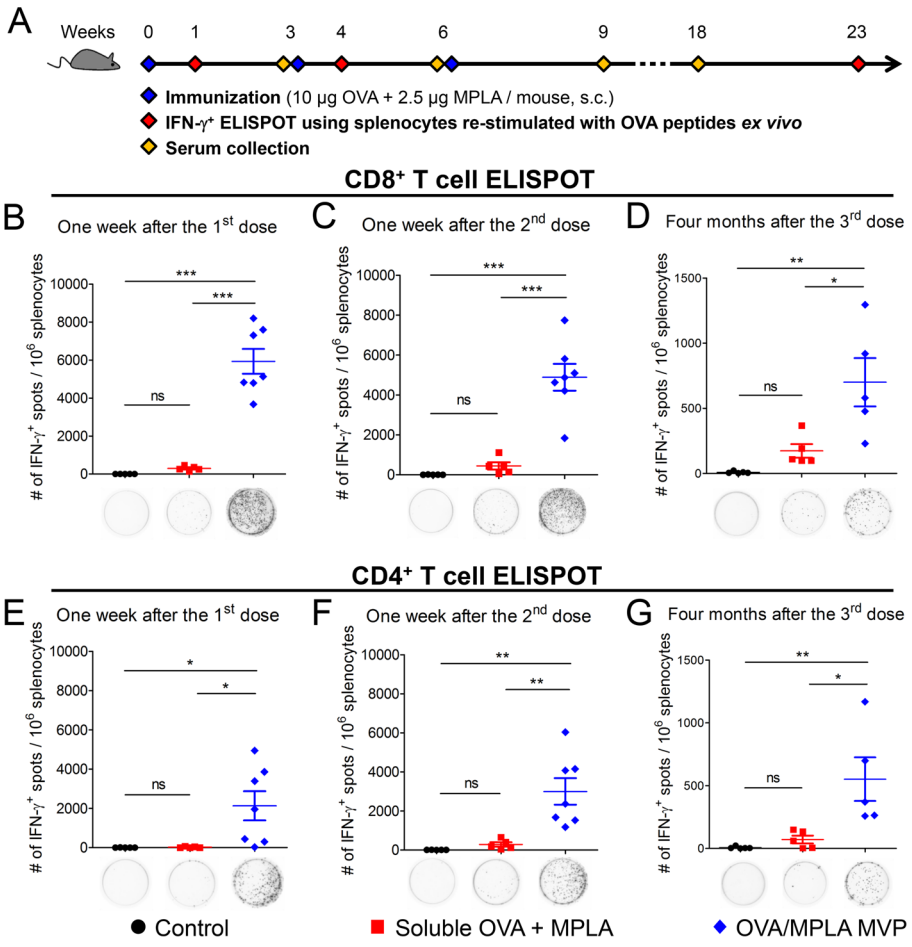

Figure 5. MVP vaccination elicits robust and durable antigen-specific T cell responses *in vivo*. (A) Immunization scheme. C57BL/6 mice were immunized subcutaneously at the tail base on weeks 0, 3, and 6 with PBS, soluble OVA and MPLA, or OVA/MPLA MVPs. Each dose contained 10 μg of OVA and 2.5 μg of MPLA/mouse. At 1 week after the (B, E) first and (C, F) second vaccination and (D, G) four months after the third vaccination, splenocytes were used in ELISPOT assays. Splenocytes were restimulated *ex vivo* with (B–D) $OVA_{257–264}$ or (E–G) $OVA_{323–339}$ peptide for quantification of IFN-γ^+CD8^+ or IFN-γ^+CD4^+ T cells, respectively. Results are presented as mean ± SEM, (B, C, E, F) n = 5–7, or (D, G) n = 5. Representative images of individual wells are shown. *P < 0.05, **P < 0.01, ***P < 0.001, analyzed by one-way ANOVA with the Bonferroni multiple comparison post-test.

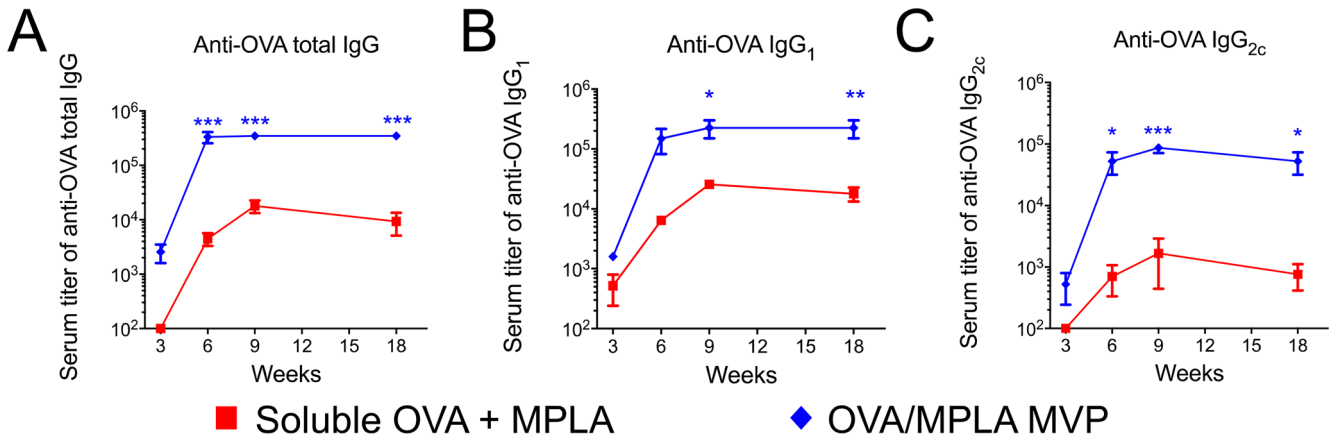

Figure 6. MVP vaccination induces potent humoral immune responses *in vivo*. C57BL/6 mice were immunized as in Figure 5A. Sera were collected after 3 weeks of each vaccination and 3 months after the third dose. Serum samples were quantified with ELISA for measuring serum titers of anti-OVA (A) total IgG, (B) IgG_1, and (C) IgG_{2c}. Results are presented as mean ± SEM, n = 5. *P < 0.05, **P < 0.01, ***P < 0.001, analyzed by two-way ANOVA with the Bonferroni multiple comparison post-test.

In parallel, we examined the immunized animals for $CD4^+$ T cell responses. Vaccination with OVA/MPLA MVPs elicited substantially greater OVA-II-specific $CD4^+$ T cell responses, compared with the soluble vaccine group (Figure 5E,F), as shown by 82-fold and 10.6-fold higher IFN-γ^+ ELISPOT counts after the first (P < 0.05) and second (P < 0.01)

DOI: 10.1021/acsnano.9b03660
ACS Nano XXXX, XXX, XXX–XXX

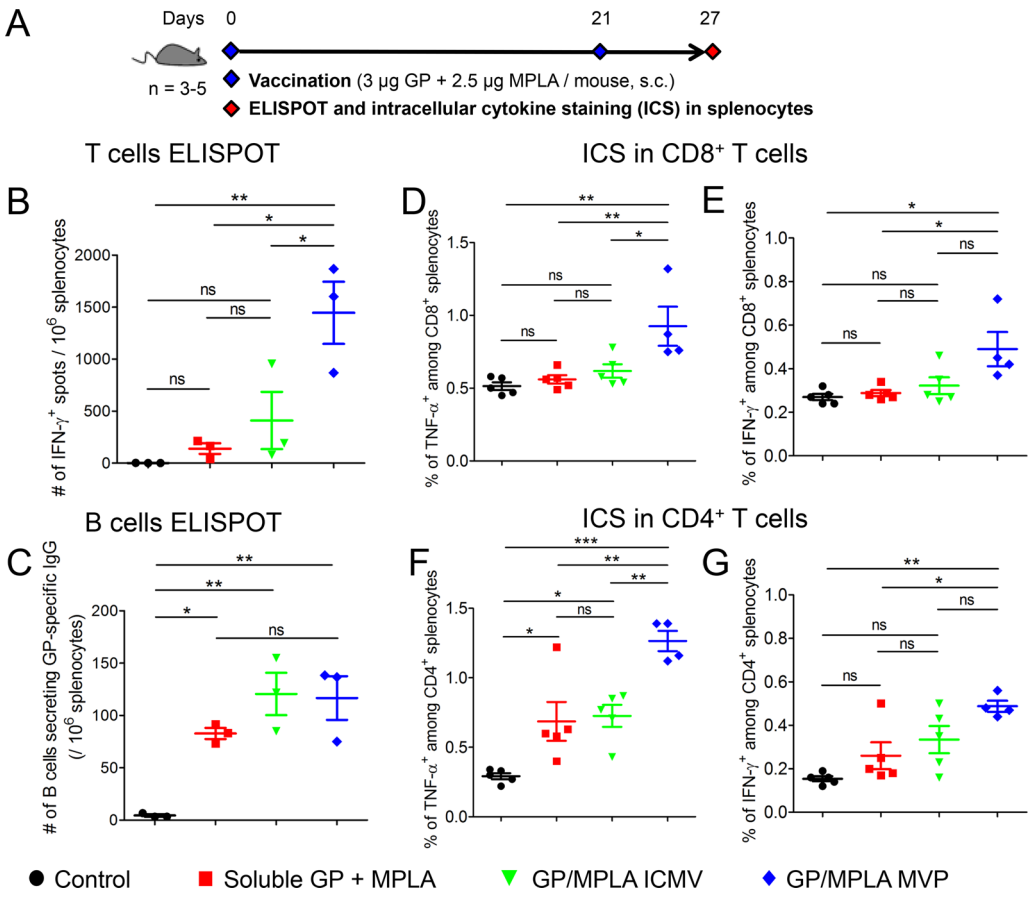

Figure 7. MVP vaccination generates strong EBOV GP-specific immune responses. (A–G) C57BL/6 mice were immunized subcutaneously with soluble GP + MPLA, GP/MPLA ICMVs, or GP/MPLA MVPs on days 0 and 21. At 1 week after the final dose, splenocytes were collected and restimulated *ex vivo* for quantification of antigen-specific (B) IFN-γ^+ T cells or (C) B cells by ELISPOT. (D–G) Intracellular cytokine staining was performed to quantitate the percentage of (D, F) IFN-γ+ and (E, G) TNF-α^+ T cells among (D, E) CD8$^+$ and (F, G) CD4$^+$ T cells. Results are presented as mean ± SEM, (B, C) n = 3 and (D, E, F, G) n = 4, 5. *P < 0.05, **P < 0.01, ***P < 0.001, analyzed by one-way ANOVA with the Bonferroni multiple comparison post-test.

vaccination, respectively. In addition, an ELISPOT assay performed at 4 months after the third vaccination showed that MVP immunization sustained markedly stronger antigen-specific CD4$^+$ T cell responses, as demonstrated by a 7.8-fold greater average number of ELISPOT counts, compared with the soluble vaccine (P < 0.05, Figure 5G). We sought to further examine induction of antigen-specific CD4$^+$ T cell activation by MVPs. BMDCs pulsed *in vitro* with OVA/MPLA MVPs significantly enhanced the proliferation of OT-II CD4$^+$ T cells with a T cell receptor (TCR) specific for the $OVA_{323-339}$ peptide (sequence: ISQAVHAAHAEINEAGR), compared with the soluble OVA + MPLA mixture (P < 0.001, Figure S7A). To validate these results *in vivo*, we adoptively transferred OT-II CD4$^+$ T cells expressing a CD45.2$^+$ congenic marker into CD45.1$^+$ recipient mice on day 0, followed by vaccination on day 1 with OVA and MPLA in either soluble or MVP form (Figure S7B). Analysis of transferred CD45.2$^+$ T cells in the spleen on day 8 showed that OVA/MPLA MVPs significantly induced proliferation of OVA-specific OT-II CD4$^+$ T cells, compared with the soluble vaccine (P < 0.001, Figure S7C).

Taken altogether, these results demonstrated that MVP vaccination markedly improved T cell immune responses, compared with vaccination with the soluble mixture. In particular, OVA/MPLA MVPs achieved robust antigen-specific T cell responses, characterized by balanced CD8+ and CD4+ T cell responses that were maintained even after 4 months of vaccination. This highlights the potency of MVP vaccination for eliciting robust and durable T cell immune responses with subunit protein antigens.

Nanoparticle Vaccines Elicit Robust Humoral Immune Responses. We also examined humoral immune responses induced by vaccination with OVA/MPLA MVPs. Following the immunization scheme shown in Figure 5A, we immunized animals, collected serum at week 3 after each vaccination, and quantified anti-OVA total IgG, IgG_1, and IgG_{2c} serum titers. Compared with soluble vaccination, OVA/MPLA MPV vaccination achieved a 19-fold higher level of anti-OVA serum IgG by 9 weeks (P < 0.001, Figure 6A) and maintained robust antibody responses throughout 18 weeks (P < 0.001, Figure 6A). Analysis of antibody subtypes indicated that compared with soluble vaccination, MVP vaccination induced 9-fold (P < 0.05) and 13-fold (P < 0.01) higher levels of anti-OVA IgG_1 serum titers by weeks 9 and 18, respectively (Figure 6B). Similarly, MVP vaccination elicited 52-fold (P < 0.001) and 69-fold (P < 0.05) higher levels of anti-OVA IgG_{2c} serum titers than soluble vaccination on weeks 9 and 18, respectively (Figure 6C). These data indicated that MVP vaccination generated robust, Th_1/Th_2-balanced humoral immune responses.

DOI: 10.1021/acsnano.9b03660
ACS Nano XXXX, XXX, XXX–XXX

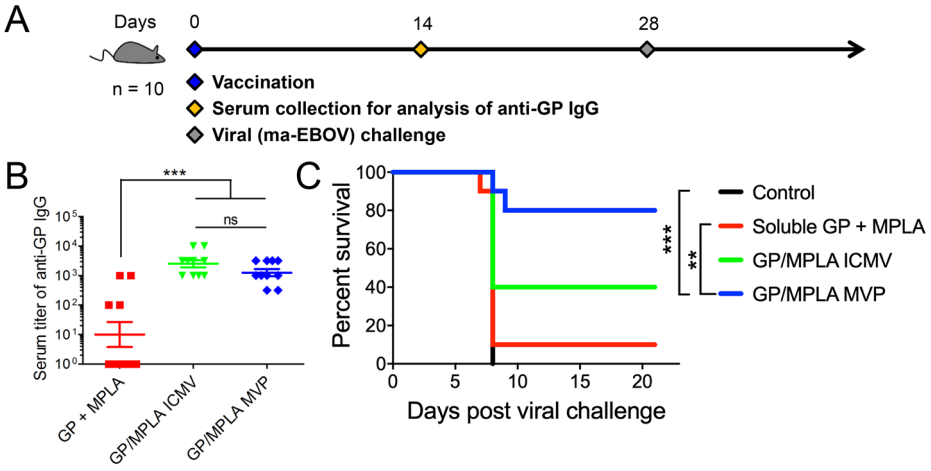

Figure 8. MVP vaccination protects mice against lethal EBOV infection. (A–C) C57BL/6 mice (n = 10) were immunized subcutaneously on day 0 with a single dose of GP and MPLA formulated in MVPs or ICMVs (3 μg of GP and 2.5 μg of MPLA) or as a soluble mixture (10 μg of GP + 2.5 μg of MPLA). (B) Sera collected on day 14 were assessed for GP-specific IgG serum titers by ELISA. (C) Preimmunized mice were inoculated intraperitoneally on day 28 with a lethal dose (1000 pfu) of mouse-adapted EBOV and monitored for animal survival. Results are presented as mean ± SEM, n = 10. (B) ***P < 0.001, analyzed by one-way ANOVA with the Bonferroni multiple comparison post-test. (C) **P < 0.01, ***P < 0.001, analyzed by the log-rank (Mantel–Cox) test.

GP/MPLA Co-loaded MVP Induced Strong Vaccine Efficacy against EBOV. Based on the compelling immunogenicity results of MVP vaccination, we assessed the MVP platform for vaccination against EBOV. In particular, we synthesized MVPs carrying an EBOV GP antigen, which is a recombinant protein antigen derived from the EBOV viral spike glycoprotein.[22] We incorporated GP and MPLA into MVPs using the same protocol as presented above and analyzed antigen-specific T cell immune responses after immunizations on days 0 and 21 (Figure 7A). In addition, we directly compared MVPs to our previously reported multilamellar lipid nanosystem formed by cross-linking of lipid layers using a bifunctional cross-linker (termed ICMVs).[13] For assessing T cell immunity, we performed *ex vivo* restimulation of splenocytes with WE15 (WIPYFGPAAE-GIYTE), a GP-specific peptide with epitopes for both major histocompatibility complex (MHC)-I and -II. GP/MPLA MVPs markedly enhanced GP-specific T cell responses, as shown by 10-fold and 3.5-fold greater IFN-γ^+ ELISPOT counts, compared with the soluble and ICMV vaccine groups, respectively (P < 0.05, Figure 7B). More specifically, intracellular cytokine staining for IFN-γ and TNF-α indicated that GP/MPLA MVP vaccination significantly increased GP-specific, polyfunctional $CD8^+$ and $CD4^+$ T cell responses, compared with the soluble vaccine (P < 0.05, Figure 7D–G). All vaccine groups increased GP-specific B cell frequencies, but there was no statistical difference among the vaccine groups (Figure 7C).

Having demonstrated immunogenicity of GP/MPLA MVPs, we examined their efficacy to protect animals against EBOV viral infection. As there is an urgent need to develop rapid yet durable countermeasures against bioterrorism agents,[12] we employed a rigorous test model where animals were challenged with a lethal dose (1000 particle forming units) of mouse-adapted EBOV on day 28 after a single-dose vaccination with 3 μg of GP (Figure 8A). A single dose of MVP vaccination significantly enhanced GP-specific IgG serum titers, achieving on average 128-fold higher serum titers compared with soluble GP + MPLA vaccination (P < 0.001, Figure 8B). Importantly, a single-dose MVP vaccination protected 80% of animals against EBOV viral challenge, whereas soluble vaccination protected only 10% of animals (P < 0.01, Figure 8C). While a single-dose ICMV vaccination also induced robust GP-specific IgG serum titers, ICMVs protected only 40% of animals (Figure 8B,C), suggesting that concerted T cell and IgG responses elicited by MVPs (Figure 7B–G, Figure 8B) may have contributed to their strong efficacy. Overall, these results demonstrated that MVP vaccination elicited protective immunity against lethal EBOV exposure.

In this work, we have demonstrated the general applicability of MVPs using both a model antigen OVA and an EBOV subunit antigen. In particular, immunizations with GP/MPLA MVPs elicited strong GP-specific adaptive immune responses (Figure 7), and a single MVP vaccination with a 3 μg GP dose exhibited an impressive 80% protection rate against lethal EBOV exposure given at 4 weeks postvaccination (Figure 8), thus demonstrating protection against ma-EBOV infection under dose-sparing conditions of a recombinant EBOV GP antigen. It is difficult to make direct comparisons between our EBOV study results and those of other previous EBOV vaccine strategies due to differences in vaccine schedules, modalities, and dose. Nevertheless, prior studies have reported protective immunity against EVD in rodent models with a recombinant EBOV GP fused to human IgG_1 Fc formulated with adjuvant;[32,33] however, they achieved protection after prime–boost–boost vaccination with a GP antigen dose of 25–100 μg.[32,33] Similarly, prime–boost–boost immunizations with 10 μg of EBOV GP mixed with a proprietary saponin-based TLR4 agonist or a complex squalene-based emulsion have been reported to protect mice against a lethal EBOV exposure.[24,34] However, it remains to be tested if such previous approaches would offer a single-dose protection against EBOV infection with low antigen dose as in our current MVP EBOV studies.

Despite extensive research in the field of Filoviruses, immune correlates of protection against EVD are largely unknown.[5,6] Nevertheless, detailed rodent and nonhuman primate studies suggest that both potent EBOV GP-specific humoral immunity and $CD4^+$ and $CD8^+$ T cell responses are required for complete protection.[35–39] On the basis of these

DOI: 10.1021/acsnano.9b03660
ACS Nano XXXX, XXX, XXX–XXX

findings and our immunogenicity data, we speculate that robust, concerted humoral and cellular immune responses elicited by MVP vaccination collectively contributed to the protective immunity against EBOV infection observed in our proof-of-concept studies. Further studies are needed to delineate the mechanisms of action for MVP vaccination.

MATERIALS AND METHODS

Materials. Lipids including DOPC, DOTAP, and MPLA were purchased from Avanti Polar Lipids. The maleimide-modified lipid DOBAQ-MAL and HA-SH were synthesized as described previously.[40] Ovalbumin was from Worthington Biochemical Corporation, DQ-OVA was from ThermoFisher Scientific, and the Ebola glycoprotein was kindly provided by Dr. Christopher L. Cooper (USAMRIID). All other materials were at least reagent grade.

Synthesis and Characterization of MVPs. Lipids composed of DOTAP, DOPC, and DOBAQ-MAL (1:0.5:0.5, m/m) plus MPLA were dried to form the lipid film, which was then hydrated with proteins (50 μg of OVA or 40 μg of GP/1.26 μmol of total lipids) dissolved in PBS buffer (pH 7.4) at room temperature for 1 h under intermittent vortex, followed by brief sonication, addition of HA-SH (200 μg/1.26 μmol of total lipids), and incubation at 37 °C for 1 h under 700 rpm constant shaking to promote complexation and cross-linking. The resulting particles were washed with PBS by centrifuging (20817*g*, 5 min) three times, dispersed by brief sonication, and stored at 4 °C before use. ICMVs coloaded with GP and MPLA were synthesized as reported previously.[13]

Particle size and surface charge were measured by dynamic laser scattering (DLS) using the Zetasizer Nano (Malvern, UK). Particle morphology was visualized by transmission electron microscopy (TEM). In brief, drops of nanoparticle solution were adsorbed for 1 min to a glow discharged 400-mesh copper grid covered with carbon-coated colloidion film (Structure Probe, Inc.). The grids were washed twice with deionized water and then negatively stained in 0.7% uranyl formate. TEM images were obtained on a FEI Morgagni electron microscope run at 100 keV and a magnification of 22 000× (2.1 Å/pixel) and then recorded on a Gatan Orius charge-coupled device camera.

The encapsulation efficiency of proteins was measured by SDS-PAGE followed by Coomassie Blue staining. The lamellarity of MVPs was measured as previously described.[26] *In vitro* leakage of the encapsulated protein antigen was measured by a fluorescence-based assay. In brief, particles loaded with Alexa Fluor 647-labeled OVA (OVA-AF647) or soluble OVA-AF647 (control) were added into a 300 kDa MWCO dialysis tube (Spectrum G235060) and incubated in PBS supplemented with 10% FBS at 37 °C under 120 rpm constant shaking. Samples outside the dialysis tube were collected at predetermined time points within 1 week and quantified for fluorescence intensity using a plate reader (Synergy Neo, BioTek, USA). The protein release was also examined under detergent treatments. Briefly, OVA-AF647-loaded MVPs and liposomes (composed of the same lipids as in MVPs) were treated by different concentrations of Triton X-100 in PBS and analyzed for protein release immediately or after incubation for 6 h at 37 °C. The percent release was calculated by dividing the fluorescence intensity of the supernatant by the total fluorescence intensity after complete disruption of particles with 1% Triton X-100 in PBS.

To determine the display of proteins on the surfaces of MVPs, OVA-loaded and DiD-labeled (0.1% mol of total lipids) particles were stained by an anti-OVA-FITC antibody (Abcam ab85584, 1:100 dilution) at room temperature for 1 h, followed by multiple washes using an airfuge (200000*g*, 10 min). The pellet was resuspended in 1% Triton PBS and measured for the fluorescence intensity at Ex/Em = 488/520 (FITC) nm and 650/680 nm (DiD) using a plate reader. Ebola GP-loaded particles were first stained with a primary antibody (mouse-13C6, provided by Dr. Christopher L. Cooper, USAMRIID, 1:100 dilution), followed by washes and staining with a goat anti-mouse IgG-PE secondary antibody (eBioscience 12-4010-87, 1:50 dilution), and measured for the fluorescence intensity as above. In a separate study, the specificity of the primary antibody was determined by staining DiD-labeled and GP-loaded MVPs with 13C6 or an isotype control antibody, followed by the same sample processing as above.

Activation of BMDCs *in Vitro*. Murine bone-marrow-derived dendritic cells were prepared according to a previous protocol[41] and used within days 7−11 of culture. DCs were seeded into a 24-well plate at 2×10^5 cells/well and treated with soluble MPLA or MVPs with or without MPLA loading at 0.5 μg/mL MPLA for 24 h. Cells were then collected and measured for the expression of CD80 (eBioscience 12-0801) by flow cytometry (CytoFLEX, Beckman Coulter, USA). Cell culture supernatant was also collected for the measurement of DC secretion of TNF-α by ELISA.

Uptake and Intracellular Processing of Protein Antigens by BMDCs *in Vitro*. For the antigen uptake study, BMDCs were seeded into a 24-well plate at 2×10^5 cells/well and incubated with soluble OVA-AF647 or OVA-AF647 MVPs at 0.8 μg of protein/mL for 2 or 24 h, followed by the measurement of fluorescence intensity among $CD11c^+$ (BD558079) DCs by flow cytometry. To investigate the intracellular processing of protein antigens, MVPs were loaded with MPLA and DQ-OVA (OVA labeled with a self-quenched fluorescent probe, which will fluoresce upon protein degradation) and added to the DC culture at a dose of 2 μg of DQ-OVA and 0.25 μg of MPLA/2×10^5 cells, followed by an incubation for 24 h and measurement of fluorescence intensity in DCs by flow cytometry. The soluble mixture of DQ-OVA and MPLA was also included as a control. For the confocal microscopy study, DCs were seeded on glass coverslips put into a 24-well plate and incubated with the soluble mixture of DQ-OVA and MPLA or DQ-OVA/MPLA coloaded MVPs at 1 μg of DQ-OVA and 0.2 μg of MPLA/2×10^5 cells for 24 h, followed by washes and staining of cells with 0.1 μM Lysotracker (ThermoFisher L7528) and 1 μg/mL Hoechst 33342 (ThermoFisher H3570) at 37 °C for 1 h. Cells were then fixed using 4% paraformaldehyde solution, coated on a glass slide using the ProLong Diamond Antifade Mountant (ThermoFisher P36965), and visualized using a confocal microscope (Nikon A1, USA).

Proliferation of Antigen-Specific $CD4^+$ T Cells *ex Vivo*. BMDCs were seeded into a 96-well plate at 5×10^4 cells/well and treated with soluble OVA plus MPLA or OVA/MPLA coloaded MVPs at a series of concentrations for 4 h. OVA-specific $CD4^+$ T cells were purified from OT-II mice (kindly provided by Dr. Lonnie Shea, University of Michigan) using a EasySep kit (STEMCELL 19765), labeled with the CFSE fluorescence dye (ThermoFisher C34570), and added to the treated BMDCs at 5×10^4 cells/well. After coculture for 3 days, the proliferation of T cells was measured by dilutions of the CFSE fluorescence by flow cytometry.

Proliferation of Antigen-Specific $CD4^+$ T Cells *in Vivo*. $CD45.1^+$ C57BL/6 mice (six-week-old, female, The Jackson Laboratory, USA) were intravenously transferred with 3×10^5 naïve $CD4^+$ T cells isolated from $CD45.2^+$ OT-II mice. One day later, recipient mice were immunized with PBS, the soluble mixture of OVA and MPLA, or OVA/MPLA MVPs at 10 μg of OVA and 2 μg of MPLA/mouse. One week later, splenocytes from recipients were collected and stained with CD4 (BD 560569) and CD45.2 (BD 561874) for quantification of the percent of transferred $CD45.2^+$ cells among total $CD4^+$ splenocytes using flow cytometry.

MVP Immunization and EBOV Virus Infection Studies. Animal studies were conducted under an Institutional Animal Care and Use Committee (IACUC) approved protocol in compliance with the Animal Welfare Act, PHS Policy, and other Federal statutes and regulations. Animal experiments employing the OVA and GP antigen were performed under approval from IACUC at the University of Michigan and USAMRIID, respectively. All animal experiments were conducted at an Association for Assessment and Accreditation of Laboratory Animal Care, international accredited facility. C57BL/6 mice were immunized subcutaneously at the tail base with PBS, the soluble mixture of OVA and MPLA, or OVA/MPLA MVPs every 3 weeks for three doses. Each dose was composed of 10 μg of OVA and 2.5 μg of MPLA. At 1 week after the first and second doses and 17 weeks after the third dose, splenocytes were collected and purified

DOI: 10.1021/acsnano.9b03660
ACS Nano XXXX, XXX, XXX−XXX

using the lymphocyte separation medium (Lonza 17−829), seeded into the IFN-γ ELISPOT plate (BD 551083) at 2×10^5 cells/well, and cultured with 20 μg/mL $OVA_{257-264}$ or $OVA_{323-339}$ peptide for 18 h. IFN-γ^+ spots were measured according to the manufacturer's protocol (BD 551083). At 17 weeks after the third dose, blood was also collected for quantification of the percent of peripheral OVA-specific $CD8^+$ T cells using a SIINFEKL-$H2K^b$-PE tetramer (MBL, USA).[42] Under the same immunization scheme, sera were collected at 3 weeks after each dose and 9 weeks after the third dose for analyses of serum titers of anti-OVA total IgG, IgG_1, and IgG_{2c} by ELISA. Titers were designated as the reciprocal of the highest dilution factors with OD_{450} values at least 2 times higher than the background values obtained from the PBS immunization group.

For studies using the EBOV GP antigen, C57BL/6 mice were immunized subcutaneously at the tail base with the soluble mixture of GP and MPLA or GP/MPLA coloaded MVPs or ICMVs every 3 weeks for two doses. Each dose was composed of 3 μg of GP and 3 μg of MPLA. Splenocytes were collected at 1 week after the second dose, restimulated *ex vivo* with 4 μg/mL of a GP-derived WE15 peptide (sequence: WIPYFGPAAEGIYTE), and quantified for GP-specific IFN-γ^+ T cells or B cells by the ELISPOT assay. Restimulated splenocytes were also quantified for the percent of intracellular IFN-γ^+ or TNF-α^+ by flow cytometry. In another study, mice received a single vaccine dose, followed by serum collection 2 weeks later for the analysis of anti-GP IgG titers by ELISA. Immunized mice were infected intraperitoneally with 1000 pfu of a mouse-adapted Ebola virus/H.sapiens-tc/COD/1976/Yambuku-Mayinga (ma-EBOV) one month later and monitored for the animal survival. Studies conducted with ma-EBOV were under the maximum BSL-4 containment.

Statistical Analysis. Data were analyzed by the unpaired, two-tailed *t*-test or the one- or two-way analysis of variance (ANOVA) followed by the Bonferroni's post-test for comparison of multiple groups using Prism 5.0 (GraphPad Software). *P* values less than 0.05 were considered statistically significant. All values are presented as mean ± SEM with an indicated sample size.

CONCLUSIONS

We have developed MVPs based on lipid−hyaluronic acid hybrid nanoparticles for vaccine applications. MVPs improved antigen delivery and antigen processing by DCs, generating robust and long-lasting antigen-specific $CD8^+$ and $CD4^+$ T cell responses as well as humoral responses. A single dose of MVP vaccination protected 80% of animals against lethal EBOV infection. MVP is a promising vaccine delivery system and warrants further investigation as a vaccine platform for recombinant protein antigens.

ASSOCIATED CONTENT

Supporting Information

The Supporting Information is available free of charge on the ACS Publications website at DOI: 10.1021/acsnano.9b03660.

Antigen release from MVPs, TEM images of MVPs, analysis of antigens loaded in MVPs, SIINFEKL-tetramer staining, and OT-II proliferation induced by MVPs *in vivo* (PDF)

AUTHOR INFORMATION

Corresponding Authors

*E-mail: christopher.l.cooper8.ctr@mail.mil.

*E-mail: moonjj@umich.edu.

ORCID

Yuchen Fan: 0000-0001-7868-2919

James J. Moon: 0000-0003-2238-2372

Notes

The authors declare no competing financial interest.

ACKNOWLEDGMENTS

This work was supported in part by the NIH (R01AI127070, R01EB022563, R01CA210273, R01CA223804, and U01CA210152), MTRAC for Life Sciences Hub, Emerald Foundation, and the Defense Threat Reduction Agency (DTRACB3947, C.L.C.). J.J.M. is a Young Investigator supported by the Melanoma Research Alliance (348774), DoD/CDMRP Peer Reviewed Cancer Research Program (W81XWH-16-1-0369), and NSF CAREER Award (1553831). Y.F. is supported in part by the UM Rackham Predoctoral Fellowship. Opinions, interpretations, conclusions, and recommendations are those of the authors and are not necessarily endorsed by the Department of Defense. We acknowledge the NIH Tetramer Core Facility (contract HHSN272201300006C) for provision of MHC-I tetramers. We thank the University of Michigan Life Sciences Institute Cryo-EM facility and help from Prof. Melanie Ohi, Dr. Min Su, and Dr. Amy Bondy. The authors declare no competing financial interest.

REFERENCES

(1) Mullan, Z. The Cost of Ebola. *Lancet Glob Health* **2015**, *3*, e423.

(2) Gostin, L. O.; Hodge, J. G., Jr. Zika Virus and Global Health Security. *Lancet Infect. Dis.* **2016**, *16*, 1099−1100.

(3) Schiller, J. T.; Lowy, D. R. Understanding and Learning from the Success of Prophylactic Human Papillomavirus Vaccines. *Nat. Rev. Microbiol.* **2012**, *10*, 681−692.

(4) Henao-Restrepo, A. M.; Camacho, A.; Longini, I. M.; Watson, C. H.; Edmunds, W. J.; Egger, M.; Carroll, M. W.; Dean, N. E.; Diatta, I.; Doumbia, M.; Draguez, B.; Duraffour, S.; Enwere, G.; Grais, R.; Gunther, S.; Gsell, P. S.; Hossmann, S.; Watle, S. V.; Konde, M. K.; Keita, S.; et al. Efficacy and Effectiveness of an Rvsv-Vectored Vaccine in Preventing Ebola Virus Disease: Final Results from the Guinea Ring Vaccination, Open-Label, Cluster-Randomised Trial (Ebola Ca Suffit!). *Lancet* **2017**, *389*, 505−518.

(5) Agnandji, S. T.; Huttner, A.; Zinser, M. E.; Njuguna, P.; Dahlke, C.; Fernandes, J. F.; Yerly, S.; Dayer, J. A.; Kraehling, V.; Kasonta, R.; Adegnika, A. A.; Altfeld, M.; Auderset, F.; Bache, E. B.; Biedenkopf, N.; Borregaard, S.; Brosnahan, J. S.; Burrow, R.; Combescure, C.; Desmeules, J.; et al. Phase 1 Trials of Rvsv Ebola Vaccine in Africa and Europe. *N. Engl. J. Med.* **2016**, *374*, 1647−1660.

(6) Regules, J. A.; Beigel, J. H.; Paolino, K. M.; Voell, J.; Castellano, A. R.; Hu, Z.; Munoz, P.; Moon, J. E.; Ruck, R. C.; Bennett, J. W.; Twomey, P. S.; Gutierrez, R. L.; Remich, S. A.; Hack, H. R.; Wisniewski, M. L.; Josleyn, M. D.; Kwilas, S. A.; Van Deusen, N.; Mbaya, O. T.; Zhou, Y.; et al. A Recombinant Vesicular Stomatitis Virus Ebola Vaccine. *N. Engl. J. Med.* **2017**, *376*, 330−341.

(7) Ura, T.; Okuda, K.; Shimada, M. Developments in Viral Vector-Based Vaccines. *Vaccines (Basel, Switz.)* **2014**, *2*, 624−641.

(8) Locher, S.; Schweneker, M.; Hausmann, J.; Zimmer, G. Immunogenicity of Propagation-Restricted Vesicular Stomatitis Virus Encoding Ebola Virus Glycoprotein in Guinea Pigs. *J. Gen. Virol.* **2018**, *99*, 866−879.

(9) McWilliams, I. L.; Kielczewski, J. L.; Ireland, D. D. C.; Sykes, J. S.; Lewkowicz, A. P.; Konduru, K.; Xu, B. C.; Chan, C. C.; Caspi, R. R.; Manangeeswaran, M.; Verthelyi, D. Pseudovirus Rvsvdeltag-Zebov-Gp Infects Neurons in Retina and Cns, Causing Apoptosis and Neurodegeneration in Neonatal Mice. *Cell Rep.* **2019**, *26*, 1718−1726 e4.

(10) Irvine, D. J.; Hanson, M. C.; Rakhra, K.; Tokatlian, T. Synthetic Nanoparticles for Vaccines and Immunotherapy. *Chem. Rev.* **2015**, *115*, 11109−11146.

(11) Fan, Y.; Moon, J. J. Nanoparticle Drug Delivery Systems Designed to Improve Cancer Vaccines and Immunotherapy. *Vaccines (Basel, Switz.)* **2015**, *3*, 662−685.

DOI: 10.1021/acsnano.9b03660
ACS Nano XXXX, XXX, XXX−XXX

(12) Fan, Y.; Moon, J. J. Particulate Delivery Systems for Vaccination against Bioterrorism Agents and Emerging Infectious Pathogens. *Wiley Interdiscip Rev. Nanomed Nanobiotechnol* **2017**, *9*, 1−26.
(13) Moon, J. J.; Suh, H.; Bershteyn, A.; Stephan, M. T.; Liu, H. P.; Huang, B.; Sohail, M.; Luo, S.; Um, S. H.; Khant, H.; Goodwin, J. T.; Ramos, J.; Chiu, W.; Irvine, D. J. Interbilayer-Crosslinked Multilamellar Vesicles as Synthetic Vaccines for Potent Humoral and Cellular Immune Responses. *Nat. Mater.* **2011**, *10*, 243−251.
(14) Moon, J. J.; Suh, H.; Li, A. V.; Ockenhouse, C. F.; Yadava, A.; Irvine, D. J. Enhancing Humoral Responses to a Malaria Antigen with Nanoparticle Vaccines That Expand Tfh Cells and Promote Germinal Center Induction. *Proc. Natl. Acad. Sci. U. S. A.* **2012**, *109*, 1080−1085.
(15) Li, A. V.; Moon, J. J.; Abraham, W.; Suh, H.; Elkhader, J.; Seidman, M. A.; Yen, M.; Im, E. J.; Foley, M. H.; Barouch, D. H.; Irvine, D. J. Generation of Effector Memory T Cell-Based Mucosal and Systemic Immunity with Pulmonary Nanoparticle Vaccination. *Sci. Transl. Med.* **2013**, *5*, 204ra130.
(16) Bazzill, J. D.; Stronsky, S. M.; Kalinyak, L. C.; Ochyl, L. J.; Steffens, J. T.; van Tongeren, S. A.; Cooper, C. L.; Moon, J. J. Vaccine Nanoparticles Displaying Recombinant Ebola Virus Glycoprotein for Induction of Potent Antibody and Polyfunctional T Cell Responses. *Nanomedicine* **2019**, *18*, 414−425.
(17) Bazzill, J. D.; Ochyl, L. J.; Giang, E.; Castillo, S.; Law, M.; Moon, J. J. Interrogation of Antigen Display on Individual Vaccine Nanoparticles for Achieving Neutralizing Antibody Responses against Hepatitis C Virus. *Nano Lett.* **2018**, *18*, 7832−7838.
(18) Fan, Y.; Sahdev, P.; Ochyl, L. J.; Akerberg, J.; Moon, J. J. Cationic Liposome-Hyaluronic Acid Hybrid Nanoparticles for Intranasal Vaccination with Subunit Antigens. *J. Controlled Release* **2015**, *208*, 121−129.
(19) Beasley, K. L.; Weiss, M. A.; Weiss, R. A. Hyaluronic Acid Fillers: A Comprehensive Review. *Facial Plast. Surg.* **2009**, *25*, 86−94.
(20) Kaczanowska, S.; Joseph, A. M.; Davila, E. Tlr Agonists: Our Best Frenemy in Cancer Immunotherapy. *J. Leukocyte Biol.* **2013**, *93*, 847−863.
(21) Vacchelli, E.; Galluzzi, L.; Eggermont, A.; Fridman, W. H.; Galon, J.; Sautes-Fridman, C.; Tartour, E.; Zitvogel, L.; Kroemer, G. Trial Watch: Fda-Approved Toll-Like Receptor Agonists for Cancer Therapy. *OncoImmunology* **2012**, *1*, 894−907.
(22) Cazares, L. H.; Ward, M. D.; Brueggemann, E. E.; Kenny, T.; Demond, P.; Mahone, C. R.; Martins, K. A.; Nuss, J. E.; Glaros, T.; Bavari, S. Development of a Liquid Chromatography High Resolution Mass Spectrometry Method for the Quantitation of Viral Envelope Glycoprotein in Ebola Virus-Like Particle Vaccine Preparations. *Clin. Proteomics* **2016**, *13*, 18.
(23) Ji, Y.; Lu, Y.; Yan, Y.; Liu, X.; Su, N.; Zhang, C.; Bi, S.; Xing, X. H. Design of Fusion Proteins for Efficient and Soluble Production of Immunogenic Ebola Virus Glycoprotein in Escherichia Coli. *Biotechnol. J.* **2018**, *13*, No. e1700627.
(24) Bengtsson, K. L.; Song, H.; Stertman, L.; Liu, Y.; Flyer, D. C.; Massare, M. J.; Xu, R. H.; Zhou, B.; Lu, H.; Kwilas, S. A.; Hahn, T. J.; Kpamegan, E.; Hooper, J.; Carrion, R., Jr.; Glenn, G.; Smith, G. Matrix-M Adjuvant Enhances Antibody, Cellular and Protective Immune Responses of a Zaire Ebola/Makona Virus Glycoprotein (Gp) Nanoparticle Vaccine in Mice. *Vaccine* **2016**, *34*, 1927−1935.
(25) Martins, K.; Carra, J. H.; Cooper, C. L.; Kwilas, S. A.; Robinson, C. G.; Shurtleff, A. C.; Schokman, R. D.; Kuehl, K. A.; Wells, J. B.; Steffens, J. T.; van Tongeren, S. A.; Hooper, J. W.; Bavari, S. Cross-Protection Conferred by Filovirus Virus-Like Particles Containing Trimeric Hybrid Glycoprotein. *Viral Immunol.* **2015**, *28*, 62−70.
(26) Girard, P.; Pecreaux, J.; Lenoir, G.; Falson, P.; Rigaud, J. L.; Bassereau, P. A New Method for the Reconstitution of Membrane Proteins into Giant Unilamellar Vesicles. *Biophys. J.* **2004**, *87*, 419−429.
(27) Shedlock, D. J.; Bailey, M. A.; Popernack, P. M.; Cunningham, J. M.; Burton, D. R.; Sullivan, N. J. Antibody-Mediated Neutralization of Ebola Virus Can Occur by Two Distinct Mechanisms. *Virology* **2010**, *401*, 228−235.
(28) Wilson, J. A.; Hevey, M.; Bakken, R.; Guest, S.; Bray, M.; Schmaljohn, A. L.; Hart, M. K. Epitopes Involved in Antibody-Mediated Protection from Ebola Virus. *Science* **2000**, *287*, 1664−1666.
(29) Heesters, B. A.; van der Poel, C. E.; Das, A.; Carroll, M. C. Antigen Presentation to B Cells. *Trends Immunol.* **2016**, *37*, 844−854.
(30) Blum, J. S.; Wearsch, P. A.; Cresswell, P. Pathways of Antigen Processing. *Annu. Rev. Immunol.* **2013**, *31*, 443−473.
(31) Gao, J.; Ochyl, L. J.; Yang, E.; Moon, J. J. Cationic Liposomes Promote Antigen Cross-Presentation in Dendritic Cells by Alkalizing the Lysosomal Ph and Limiting the Degradation of Antigens. *Int. J. Nanomed.* **2017**, *12*, 1251−1264.
(32) Konduru, K.; Bradfute, S. B.; Jacques, J.; Manangeeswaran, M.; Nakamura, S.; Morshed, S.; Wood, S. C.; Bavari, S.; Kaplan, G. G. Ebola Virus Glycoprotein Fc Fusion Protein Confers Protection against Lethal Challenge in Vaccinated Mice. *Vaccine* **2011**, *29*, 2968−2977.
(33) Konduru, K.; Shurtleff, A. C.; Bradfute, S. B.; Nakamura, S.; Bavari, S.; Kaplan, G. Ebolavirus Glycoprotein Fc Fusion Protein Protects Guinea Pigs against Lethal Challenge. *PLoS One* **2016**, *11*, No. e0162446.
(34) Lehrer, A. T.; Wong, T. S.; Lieberman, M. M.; Humphreys, T.; Clements, D. E.; Bakken, R. R.; Hart, M. K.; Pratt, W. D.; Dye, J. M. Recombinant Proteins of Zaire Ebolavirus Induce Potent Humoral and Cellular Immune Responses and Protect against Live Virus Infection in Mice. *Vaccine* **2018**, *36*, 3090−3100.
(35) Marzi, A.; Engelmann, F.; Feldmann, F.; Haberthur, K.; Shupert, W. L.; Brining, D.; Scott, D. P.; Geisbert, T. W.; Kawaoka, Y.; Katze, M. G.; Feldmann, H.; Messaoudi, I. Antibodies Are Necessary for Rvsv/Zebov-Gp-Mediated Protection against Lethal Ebola Virus Challenge in Nonhuman Primates. *Proc. Natl. Acad. Sci. U. S. A.* **2013**, *110*, 1893−1898.
(36) Martins, K. A. O.; Cooper, C. L.; Stronsky, S. M.; Norris, S. L. W.; Kwilas, S. A.; Steffens, J. T.; Benko, J. G.; van Tongeren, S. A.; Bavari, S. Adjuvant-Enhanced Cd4 T Cell Responses Are Critical to Durable Vaccine Immunity. *EBioMedicine* **2016**, *3*, 67−78.
(37) Warfield, K. L.; Olinger, G. G. Protective Role of Cytotoxic T Lymphocytes in Filovirus Hemorrhagic Fever. *J. Biomed. Biotechnol.* **2011**, *2011*, 984241.
(38) Wong, G.; Richardson, J. S.; Pillet, S.; Patel, A.; Qiu, X.; Alimonti, J.; Hogan, J.; Zhang, Y.; Takada, A.; Feldmann, H.; Kobinger, G. P. Immune Parameters Correlate with Protection against Ebola Virus Infection in Rodents and Nonhuman Primates. *Sci. Transl. Med.* **2012**, *4*, 158ra146.
(39) Cooper, C. L.; Martins, K. A.; Stronsky, S. M.; Langan, D. P.; Steffens, J.; Van Tongeren, S.; Bavari, S. T-Cell-Dependent Mechanisms Promote Ebola Vlp-Induced Antibody Responses, but Are Dispensable for Vaccine-Mediated Protection. *Emerging Microbes Infect.* **2017**, *6*, e46.
(40) Fan, Y.; Kuai, R.; Xu, Y.; Ochyl, L. J.; Irvine, D. J.; Moon, J. J. Immunogenic Cell Death Amplified by Co-Localized Adjuvant Delivery for Cancer Immunotherapy. *Nano Lett.* **2017**, *17*, 7387−7393.
(41) Lutz, M. B.; Kukutsch, N.; Ogilvie, A. L.; Rossner, S.; Koch, F.; Romani, N.; Schuler, G. An Advanced Culture Method for Generating Large Quantities of Highly Pure Dendritic Cells from Mouse Bone Marrow. *J. Immunol. Methods* **1999**, *223*, 77−92.
(42) Ochyl, L. J.; Moon, J. J. Whole-Animal Imaging and Flow Cytometric Techniques for Analysis of Antigen-Specific Cd8+ T Cell Responses after Nanoparticle Vaccination. *J. Visualized Exp.* **2015**, No. e52771.

DOI: 10.1021/acsnano.9b03660
ACS Nano XXXX, XXX, XXX−XXX